PROC. OF JSCE
No. 341, January 1984

DYNAMIC STRENGTH CHARACTERISTICS OF AXIALLY LOADED COLUMNS SUBJECTED TO PERIODIC LATERAL ACCELERATION

By Shigeru KURANISHI and Akinori NAKAJIMA***

1. INTRODUCTION

Recently, studies on the ultimate strength of bridge structures for static loads have been extensively done and design practice have been gradually improving to that based on the limit state. However, there are many problems to be solved in order to establish the limit state design of the structures under dynamic effects such as wind forces or excitations by earthquake. Especially, the structural instability to static loads inheres in relatively slender bridge structures and the instability is expected to be enhanced by the dynamic loadings. Therefore, the dynamic behaviors of these structures in the ultimate state including the structural instability is required to be studied in order to extend the limit state design to dynamic loadings.

Up to this time, many studies on the restoring characteristics and the inelastic deformation capacities of structures have been carried out[1),2)]. Kato and Akiyama[3)~5)] discussed the dynamic ultimate strength of building structures on the basis of the concept of the input energy, where the inelastic deformation capacities were connected to the input earthquake energy. However, these studies did not sufficiently consider the dynamic instability effects on the column strength and the dynamic characteristics of other types of structure subjected to combined dynamic and static loadings. From the nature of things, the dynamic ultimate strength should be defined by the dynamic failure instead of the ultimate strength estimated by the results of experiments and analyses for static cyclic loading. To accomplish this subject, it will be necessary to clarify the ultimate state of structures under dynamic loadings according to dynamic loading experiments and/or nonlinear dynamic analyses.

Owing to the remarkable advance of computers, the dynamic analysis[6),7)] in which the geometrical and material nonlinearities are taken into consideration have been developed so far. In this analysis, the general step-by-step integration such as Newmark's β method ($\beta=1/4$) is used. However, when Newmark's β method ($\beta=1/4$) is applied to the linear dynamic analysis, the analytical errors such as the phase error are produced as well known[8)], by the reason of that the solutions are given approximately by discrete points. By applying of this method to nonlinear multi-degree-of-freedom systems, it is checked roughly here that these errors decrease with decreasing the time interval, and that this method can trace the dynamic ultimate conditions sufficiently enough.

In this paper, the dynamic ultimate strength characteristics of the compression members such as used for bridge trusses subjected to the lateral sinusoidal acceleration whose circular frequency is equal to the first natural circular frequency of the column is investigated.

Furthermore, the effect of the static axial compression force on the dynamic responses is discussed using a simplified simulation model.

2. ANALYTICAL METHOD

(1) General

The geometrical and material nonlinearities are included in the analysis using the modified Newton-Raphson method and the modified incremental load method. Firstly, the equation of the virtural work of finite deformations is derived basing on the incremental theory. Secondly, the equivalent incremental equation of motion is formulated according to the standard procedure of the finite element method. This equation of motion is solved using Newmark's β method[6),7)]. The stress-strain curve of the

* Member of JSCE, Dr. of Eng., Professor, Dept. of Civil Engineering, Tohoku University.
** Member of JSCE, Dr. of Eng., Research Associate, Civil Engineering, Tohoku University.

steel material is assumed to be the ideal elastic-plastic relationship and the elastic unloading is taken into account in the case where the stress reverse occurs. In this paper, only the effect of damping due to the hysteresis of material on the structural responses is considered, because the effect of the hysteresis damping is more remarkable than that of the other inherent structural damping for the dynamic ultimate strength.

(2) Integration of the equation of motion

The formulation of the finite deformation problems based on the incremental theory is same as used in Ref. 9). The integration process in solving the incremental equation of motion is as follows.

The dynamic force equilibrium at time t_n can be written as

$$\{I_n\}+\{R_n\}=\{F_n\} \quad \cdots\cdots(1)$$

in which $\{I_n\}$, $\{R_n\}$ and $\{F_n\}$ are inertia force, internal resisting force and external force vectors at time t_n respectively. The dynamic force equilibrium at time t_{n+1} can be obtained similarly. Therefore, the incremental equation of motion can be given by

$$\{I\}+\{R\}=\{F\} . \quad \cdots\cdots(2)$$

Hence, the incremental inertia force vector $\{I\}$ and the incremental internal resisting force vector $\{R\}$ can be approximately given as the function of the incremental displacement vector $\{D\}$ by

$$\{R\}=[K_n]\{D\} \quad \cdots\cdots(3\cdot a)$$

$$\{I\}=[M]\left(\frac{1}{\beta\Delta t^2}\{D\}-\frac{1}{\beta\Delta t^2}\{\dot{D}_n\}-\frac{1}{2\beta}\{\ddot{D}_n\}\right) \quad \cdots\cdots(3\cdot b)$$

in which $[K_n]$ is the tangent stiffness matrix at time t_n[9] and $[M]$ is the equivalent consistent mass matrix including the effect of rotary inertia[10]. $\{\dot{D}_n\}$ and $\{\ddot{D}_n\}$ are the velocity and the acceleration vectors at time t_n and Δt is the time interval from t_n to t_{n+1}. The terms parenthesized in Eq. (3·b) are derived from the formula of Newmark's β method which is generally written as

$$\{D_{n+1}\}=\{D_n\}+\Delta t\{\dot{D}_n\}+(\Delta t^2/2)\{\ddot{D}_n\}+\beta\Delta t^2(\{\ddot{D}_{n+1}\}-\{\ddot{D}_n\}) . \quad \cdots\cdots(4)$$

By substituting Eq. (3) into Eq. (2), the following expression is obtained

$$\left([K_n]+\frac{1}{\beta\Delta t^2}[M]\right)\{D\}=\{F\}-\{I^{(0)}\} \quad \cdots\cdots(5)$$

in which $\{I^{(0)}\}$ is the apparent external force and obtained by substituting $\{D\}=0$ into Eq. (3·b). By solving Eq. (5), the first incremental displacement vector $\{D^{(1)}\}$ is obtained. The first incremental internal resisting force vector $\{R^{(1)}\}$ and inertia force vector $\{I^{(1)}\}$ can be determined by using $\{D^{(1)}\}$. When these equations are substituted into Eq. (2), the out-of-balanced force results from the assumption of linearization of the relationship between the incremental external force and displacement. Therefore, the out-of-balanced force is corrected by applying the equivalent unbalanced force residual which is given as follows

$$\{\Gamma^{(1)}\}=\{F\}-\{R^{(1)}\}-\{I^{(1)}\} . \quad \cdots\cdots(6)$$

The iterative calculation is continued until the unbalanced force residual becomes nearly equal to zero. Eq. (5) is rewitten in the general form as follows

$$\left([K_n]+\frac{1}{\beta\Delta t^2}[M]\right)\{D^{(i+1)}\}=\{F\}-\{R^{(i)}\}-\{I^{(i)}\} \quad \cdots\cdots(7)$$

in which the iterative calculation is performed until $\{D^{(i+1)}\}$ becomes nearly equal to zero. **Fig. 1** shows the concept of the iterative calculation described above. Symbols of materices and vectors are omitted in this figure.

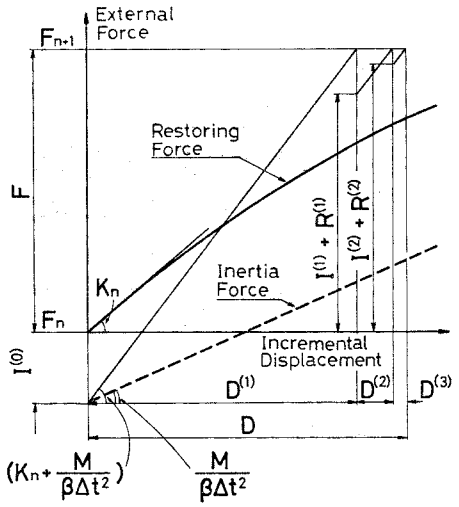

Fig. 1 Concept of iterative calculations.

3. NUMERICAL RESULTS

(1) Numerical model and parameters

Fig. 2 shows loading conditions and a cross sectional shape of columns analyzed here. The columns are simply supported and its length $l=10$ m. The applied static axial compression force P is expressed by the ratio α to the static load carrying capacity P_{cr} of the column with

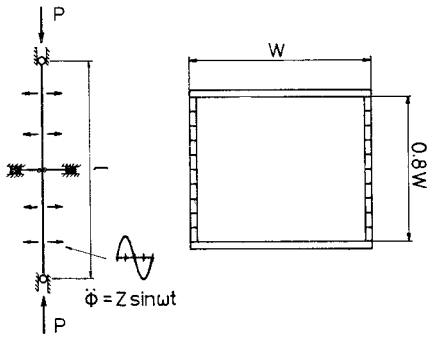

Fig. 2 Loadings and cross-section of columns.

Table 1 Characteristics of cross-section.

Slenderness Ratio	30	60	90	120	150
Flange Width (mm)	970	480	310	233	183
Thickness of Plate (mm)	23	17	21	18	14
1st Natural Circular Frequency (rad/s)	155.6	79.7	54.4	41.0	32.7
1st Natural Period (s)	0.040	0.079	0.116	0.153	0.192
Load Carrying Capacity of Column (MN)	18.30	6.24	4.08	1.79	0.75
Ratio of Load Carrying Capacity to Yield Axial Force	0.969	0.903	0.740	0.509	0.347

the initial crookedness which is given by a sinusoidal curve with the maximum magnitude at the middle being one-thousandth of the length. Therefore,

$$P=\alpha P_{cr} \quad \cdots\cdots(8)$$

In this analysis, the following cases are considered in which $\alpha=0.5$ or 0.8 and the slenderness ratio $\lambda=30$, 60, 90, 120 or 150. **Table 1** shows the width of flange, the thickness, the first natural circular frequency with no axial force, and the ratio of the load carrying capacity with the $l/1000$ initial imperfection to the yield axial force. The Young's modulus is 206 GN/m², the yield stress is 235 MN/m² and the mass per unit volume is 7.85 Mg/m³.

In the finite element analysis, the column is divided into 10 equal elements and the cross section is divided into 22 segments in order to estimate the yielded zone as shown in **Fig. 2**. The stress-strain curve is assumed to be the ideal elastic-plastic relationship and the residual stresses are neglected here.

The applied periodic lateral acceleration load is assumed to be sinusoidal and given as follows

$$\ddot{\Phi}=Z\sin\omega t \quad \cdots\cdots(9)$$

in which Z is the amplitude of the input lateral acceleration and ω is the circular frequency and taken to be equal to the first natural circular frequency of the column subjected to the axial force. Based on the obtained dynamic response of the column subjected to ten cycles of the sinusoidal acceleration, the dynamic ultimate strength characteristics is discussed here.

(2) Fundamental response characteristics

In this section, the numerical results analyzed varying the parameters of the slenderness ratio, the static axial compression force and so on are presented. **Fig. 3** shows the lateral displacement response at midheight of the column in the case where $\lambda=120$, $\alpha=0.5$ and $Z=6.0$ m/s². The ordinate shows the displacement response normalized by the column length and the abscissa is the elapse time normalized by the first natural period T_1. Since the circular frequency of the sinusoidal acceleration is equal to the first natural circular frequency of the column, the amplitude of the flexural vibration increases gradually showing resonance. And then, the yielded zone appears in the cross section at the center of the column (In **Fig. 3**, the circle shows that the initial yielding occurs). In this case, the amplitude converges to a certain magnitude and then the center of vibration begins to shift only in one direction decreasing the amplitude. The behavior that the center of vibration begins to shift only in one direction is termed herein by the increase of dynamic residual displacement. For $Z=7.0$ m/s², the displacement response increases rapidly and the column begins to collapse within ten cycles of application of the sinusoidal acceleration as shown in **Fig. 4**. After the dynamic residual displacement due to yielding of the cross section occurs, the dynamic residual displacement increases only in one direction and the amplitude decreases gradually in the same manner as the case for $Z=6.0$ m/s². But in this case, the displacement response

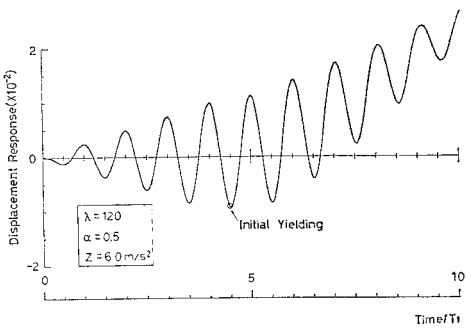

Fig. 3 Lateral displacement-time curve at midheight ($z=6.0$ m/s²).

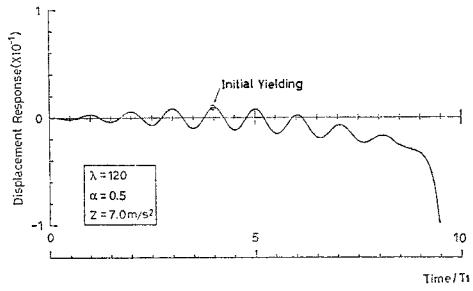

Fig. 4 Lateral displacement-time curve at midheight ($z=7.0$ m/s²).

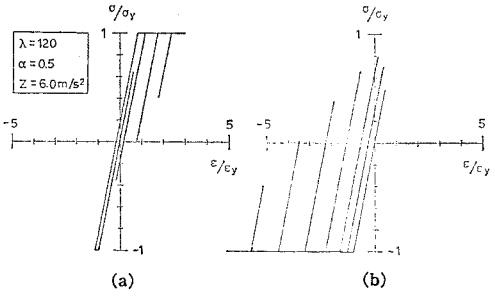

Fig. 5 Stress-strain relationships at midheight (a) Tension (b) Compression.

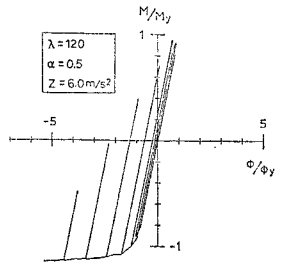

Fig. 6 Relationship between resisting bending moment and curvature at midheight.

increases rapidly and then the column collapses when the lateral displacement at midheight reaches a certain degree of value. The dynamic residual displacement increases in the opposite direction of the case for $Z=6.0$ m/s², because the flexural deformation can easily develop in the direction of the initial yielding. **Fig. 5** shows the stress-strain relationship of the cross section at midheight for $Z=6.0$ m/s². In this figure, (a) and (b) show that of the tension flange and the compression flange respectively as the result of the positive lateral deflection. The ordinate and abscissa show the stress and strain normalized by the yield stress and strain respectively. Both flanges yield first in compression because the static axial compression force is applied at its initial stage. However, as the dynamic residual displacement increases in the positive direction (upper direction in **Fig. 3**), the flange at the convex side begins to yield in tension and the plastic tension strain develops in this flange. The plastic compression strain develops in the other flange at the concave side. **Fig. 6** shows the resisting bending moment-curvature relationship at midheight of this column. The ordinate and the abscissa are the resisting bending moment and the curvature normalized by the yield moment and the yield curvature respectively. In the same manner as the stress-strain curve, the curvature develops only in one direction according to the increase of the dynamic residual displacement only in one direction.

(3) Consideration of dynamic failure characteristics

In the case of columns subjected to combined the static axial compression force and the lateral sinusoidal acceleration, the dynamic failure occurs as follows. Owing to resonance, the flexural vibration develops and the cross section in the vicinity of the midheight of the column yields. By this yielding of the cross sections, the dynamic residual displacement occurs and increases only in one direction with gradually decreasing the amplitude of the flexural vibration. If the dynamic residual displacement reaches a certain degree of value, the displacement response increases rapidly and the column collapses.

In order to debate on the mechanism of this behavior, the column is simulated here by a simplified one degree-of-freedom system subjected to the sinusoidal acceleration also shown in **Fig. 7**. This presents the flexural vibration model composed of a mass, rigid bar and rotary spring, and the mass is subjected to the vertical static load $\bar{P}$. In this figure, m is the mass, k is the rotary spring constant, $\bar{l}$ is the length of the rigid bar, y is the horizontal displacement and assumed to be much smaller than $\bar{l}$ and $f(t)$ is the external excitation. The restoring force characteristics of

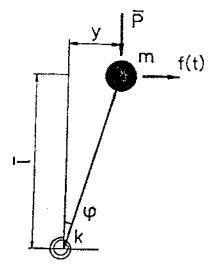

Fig. 7 One degree-of-freedom system.

the rotary spring has the ideal elastic-plastic relationship shown in **Fig. 8**. The external excitation is given by

$$f(t)=-mZ\sin\omega t \quad \cdots\cdots(10)$$

in which Z is the amplitude of the input acceleration and ω is the circular frequency of the input acceleration. The equilibrium equation of the moment with respect to the support of the vibration system shown in **Fig. 7** can be written as

$$\bar{l}m\ddot{y}+R-\bar{P}y=\bar{l}f(t) \quad \cdots\cdots(11)$$

in which R is the restoring force of the rotary spring. Depending on elastic or plastic, R can be obtained as follows

$$R=\begin{cases}\pm R_y-k(\varphi_m-\varphi) & : \text{Elastic}\\ \pm R_y & : \text{Plastic}\end{cases} \quad \cdots\cdots(12)$$

in which R_y is the yield restoring force, φ is the rotary displacement and φ_m is the standard plastic displacement introduced to estimate the restoring force shown in **Fig. 8**. By multiplying the both sides of Eq. (11) with $\dot{\varphi}$, and integrating this equation from t_1 to t_2, the following expression can be obtained by

$$\left[\frac{1}{2}m\dot{y}^2\right]_{\dot{y}_1}^{\dot{y}_2}+\int_{\varphi_1}^{\varphi_2}Rd\varphi-\frac{\bar{P}}{\bar{l}}\left[\frac{1}{2}y^2\right]_{y_1}^{y_2}=\int_{t_1}^{t_2}f(t)\dot{y}dt. \quad \cdots\cdots(13)$$

The first term is the incremental kinetic energy, the second term is the incremental strain energy and the last term is the incremental potential energy due to the static load $\bar{P}$ in the left side of Eq. (13). And the right side of Eq. (13) shows the incremental input energy due to the external excitation. It is noted that the static load $\bar{P}$ transfers its potential energy to the system, if $y_2^2>y_1^2$ and absorbes from it, if $y_2^2<y_1^2$.

Displacement response of the single degree-of-freedom system shown in **Fig. 7** are presented, using the nonlinear dynamic analysis described in chapter 2. **Fig. 9** shows a displacement response curve of the mass. The ordinate shows the displacement normalized by the length of the rigid bar and the abscissa shows the elapse time normalized by the period of external excitation. Showing resonance, the amplitude of the displacement response increases and then the rotary spring begins to yield. By the yielding, the dynamic residual displacement occurs and it increases only in one direction gradually. It is also found that the amplitude decreases when the mass moves in the opposite direction to the dynamic residual displacement. After the dynamic residual displacement reaches a certain degree of value, the displacement response increases rapidly. These behaviors agree well with the dynamic behaviors of the column subjected to the static axial compression force previously described.

Then, the equilibrium of the energy expressed in Eq. (13) will be investigated using the responses of one degree-of-freedom system. If the rotary displacement reaches the yield rotary displacement φ_y at time t_1 and the displacement begins to reverse as shown in **Fig. 9** and the velocity response is zero at this time. **Fig. 10** (a) shows the relationship between the restoring force and the rotary displacement from this time to time t_2 when the velocity response becomes zero subsequently. It is predicted that the supply of the input energy results in $|\varphi_2|>|\varphi_1|=\varphi_y$, because this system is subjected to the sinusoidal excitation at resonance. In fact, the numerical results shows that $|\varphi_2|$ is greater than φ_y. The velocity response are zero at t_1 and t_2, so that there is no

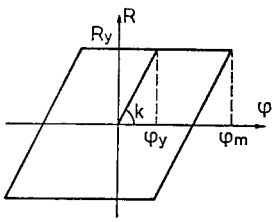

Fig. 8 Restoring force characteristics.

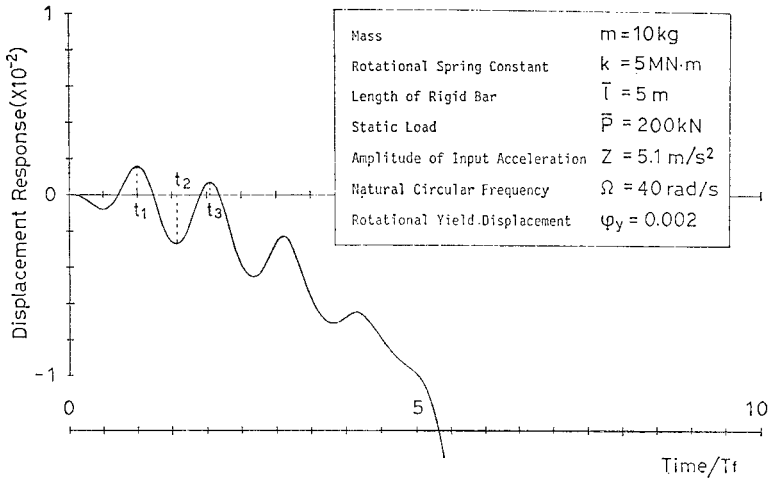

Fig. 9 Horizontal displacement-time curve.

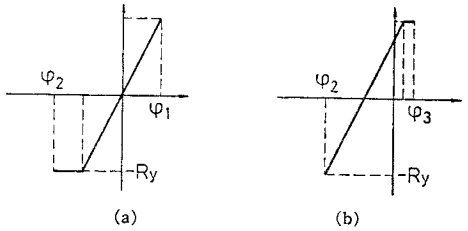

(a) (b)

Fig. 10 Relationships between restoring force and rotational displacement (a) $t_1 \sim t_2$ (b) $t_2 \sim t_3$.

increment of the kinetic energy from t_1 to t_2. Therefore, Eq. (13) can be rewritten as

$$\Delta E\varphi = \Delta E_p + \Delta E_f \quad \cdots\cdots(14)$$

in which ΔE_φ, ΔE_p and ΔE_f are the incremental strain energy, potential energy due to the static load and input energy due to the external excitation normalized by the yield strain energy ($E_y = k\varphi_y^2/2$) respectively. According to the numerical results, $|y_2|$ is greater than $|y_1|$, consequently ΔE_p is supplied to the system. In this case, the strain energy increases and the plastic deformation develops. At this time, each value of Eq. (14) is calculated as follows

$$\Delta E\varphi = 1.377, \quad \Delta E_p = 0.370, \quad \Delta E_f = 1.009$$
$$1.377 \fallingdotseq 0.370 + 1.009 . \quad \cdots\cdots(15)$$

It will be seen that the Eq. (14) is satisfied in the range of numerical errors. The equilibrium of incremental energy from t_2 to t_3 is considered. The velocity response becomes zero at time t_3. If the reverse of the displacement response from the plastic zone occurs, the strain energy released by the rotary spring is constant and the natural period of the system becomes longer owing to yielding. Therefore, the incremental input energy due to the external excitation can not exceed the incremental input energy during t_1 and t_2. The relationship between the restoring force and the rotary displacement from t_2 to t_3 is shown in **Fig. 10** (b). By the supply of the input energy which is equal to that from t_1 to t_2, $|\varphi_3|$ becomes less than $|\varphi_2|$, so $|y_3|$ is less than $|y_2|$. This means that the incremental potential energy of the static load results in the decreasing of the strain energy of the system. Consequently, the dynamic residual displacement occurs in the direction in which the first yielding is produced. If the system displaces in the opposite direction, the potential energy of the static load makes the displacement decrease and the amplitude damped. By the numerical results, each incremental energy from t_2 to t_3 is obtained as

$$\Delta E\varphi = 0.275, \quad \Delta E_p = -0.526, \quad \Delta E_f = 0.807$$
$$0.275 \fallingdotseq -0.526 + 0.807 . \quad \cdots\cdots(16)$$

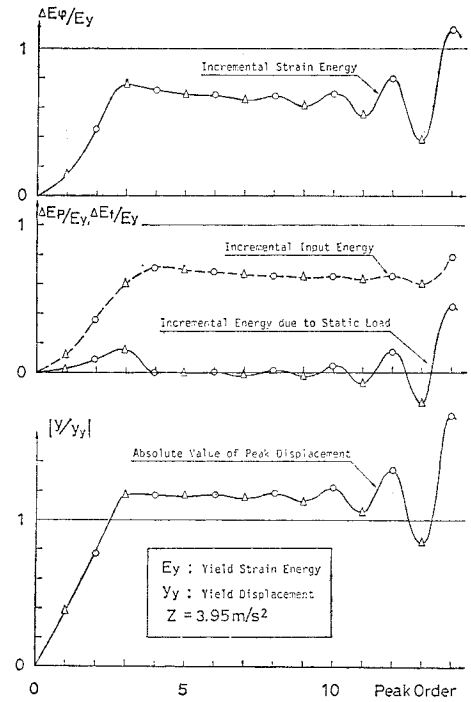

Fig. 11 Incremental energy and absolute value of horizontal displacement at every peak.

It will be seen that the static load acts as an absorber of energy in Eq. (16). **Fig. 11** shows the incremental strain energy, input energy due to the sinusoidal excitation, potential energy of the static load and the absolute peak value of the displacement response for $Z = 3.95$ m/s². The abscissa shows the order of peaks of the displacement response. The ordinate shows the incremental energy and the absolute peak value of the displacement response normalized by the yield strain energy and the yield displacement respectively. The circles give the values at the positive peak displacement and the triangles give the values at the negative one. In this figure, the first yielding occurs at the third peak. If the reverse from the plastic zone occurs, the released strain energy is constant, so the velocity response nearly holds the constant amplitude. Therefore, the incremental input energy which is expressed by the integration of the product of the sinusoidal excitation and the velocity response can not exceed a certain degree of value. The incremental input energy indicates the initial maximum point at the fourth peak and gradually decreases after that as shown in Fig. 11. This should be the reason that the natural period of the system becomes longer owing to

yielding and that the phase lag between the external excitation and the velocity response is produced. The incremental input energy decreases gradually but shows a tendency to approach a constant value. Although the absolute value of the peak displacement has a tendency to decrease as well as the above discussed, the incremental potential energy of the static load, which is related to the difference between the second power of the peak displacement responses, is supplied from the total energy of the system. This makes the strain energy and the absolute value of the peak displacement response decrease. On the contrary, it is considered that the absolute peak displacement may exceed the last peak one successively by the action of the incremental input energy which is smaller than the energy caused during the last half cycles. Therefore, the incremental potential energy of the static load is supplied to the system and makes the absolute value of the peak displacement response increase. The influence which the incremental potential energy of the static load exerts on the incremental strain energy becomes gradually significant as shown in **Fig. 11**. For the column subjected to the static axial compression force, the behavior of the dynamic residual displacement which increases only in one direction is considered to occur in the same reason.

From these considerations described above, if the system loaded by the small static load is subjected to the external excitation for a long time, the dynamic residual displacement is expected to increase only in one direction. Because, by the resonance, the amplitude of the vibration always increases and then the spring yields finally. However, in the actual structures, if the external excitation and/or the static load are relatively small, this resonance does not always induce the yielding owing to the effects of the inherent structural damping even in the elastic range. In this case, the amplitude of the vibration will become constant without the increase of the dynamic residual displacement in one direction.

In **Fig. 12**, the equilibrium of the moment caused by the static load, the inertia force and the resisting moment of the rotary spring in the previously described single degree-of-freedom system are shown by the bold solid line, the fine solid line and the dashed line respectively. The moment caused by the inertia force is including the moment by the external excitation. The total moment summed up the three moment components must be zero and the three moments are balancing at each time. The ordinate shows the moment normalized by the yield restoring force R_y and the abscissa shows the elapse time

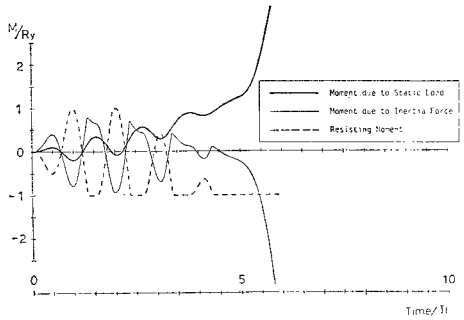

Fig. 12 Equilibrium of moment ($z=5.1$ m/s²)

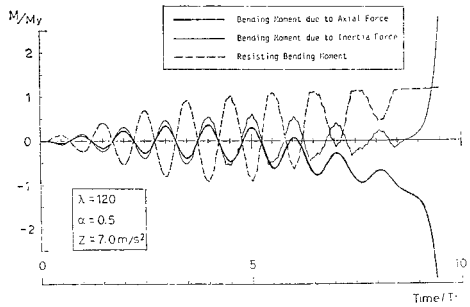

Fig. 13 Equilibrium of bending moment at midheight.

normalized by the natural period of the external excitation respectively. It will be seen that the moment caused by the static load increases rapidly when the moment nearly reaches the yield restoring force. Therefore, the critical displacement which indicates the start of the divergence of the displacement response may be given by the following condition

$$\bar{P}y > R_y \quad \cdots\cdots(17)$$

The Eq. (17) is also the static failure condition that the moment caused by the static load exceeds the maximum restoring moment of the rotary spring. This means that the displacement in the dynamic failure condition is not different from that in the static one. The equilibrium relationships between the bending moment caused by the static axial compression force, the inertia force and the bending resisting moment at midheight of the column are shown in **Fig. 13** by the similar manner as used in **Fig. 12**. This figure shows the case for the statically compressed column with the parameters $\lambda=120$, $\alpha=0.5$ and $Z=7.0$ m/s². The tendency of the behavior of the column agrees well with that of the single degree-of-freedom system shown in **Fig. 12**. Namely, the deformation of the column starts to increase quickly when the bending

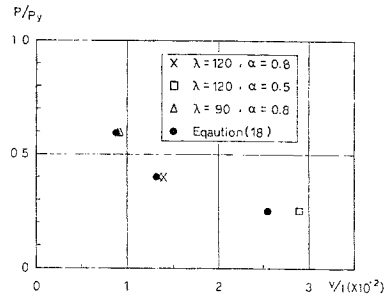

Fig. 14 Static axial load versus lateral displacement at midheight.

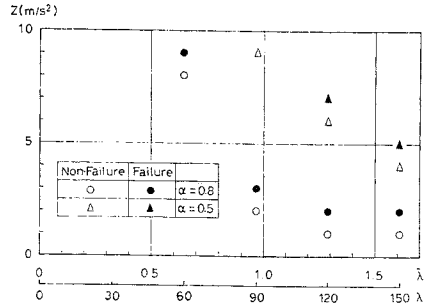

Fig. 15 Dynamic strength characteristics of columns.

moment which expresses the product of the axial force and the deflection at midheight nearly reaches the full plastic moment under the axial force. Consequently, the following expression for the column can be used in the same manner as the case of the single degree-of-freedom system

$$Pv > \bar{M}_p \quad \cdots\cdots(18)$$

It indicates that the lateral deflection at midheight in Eq. (18) gives the critical value for the divergence of deflections. Then, **Fig. 14** shows the relationships between the static axial compression force and the lateral deflection of the column at the time when the lateral deformation starts to increase rapidly in the dynamic analysis. The ordinate is the static axial compression force and the abscissa is the lateral deflection at midheight normalized by the yield axial force and the length of the column respectively. The crosses, squares and triangles show the results of the case for $\lambda=120$ and $\alpha=0.8$, $\lambda=120$ and $\alpha=0.5$, and $\lambda=90$ and $\alpha=0.8$ respectively. The black circles show the critical lateral deflection which is determined using Eq. (18) for each slenderness ratio and the static axial compression force. The critical lateral deflection given by Eq. (18) agrees well with the deflection when the deformation starts increasing rapidly in the dynamic analysis, except for $\lambda=120$ and $\alpha=0.5$. In the latter case, the discrepancy may come from the dynamic effect of the inertia force. However, this difference is smaller than about 15%.

(4) Dynamic strength characteristics of columns

By the above discussion, it may be concluded that the flexural vibration develops and the column will be brought out to collapse, when the column is subjected to combined the static axial compression force and the lateral sinusoidal acceleration whose circular frequency is equal to the first natural circular frequency of the column.

The dynamic strength of the columns in ten cycles of the sinusoidal acceleration is shown in **Fig. 15**. The ordinate shows the input acceleration amplitude as the dynamic strength of the column and the abscissa shows the slenderness ratio and slenderness ratio parameter. $\bar{\lambda}=(\pi/\lambda)\sqrt{\sigma_y/E}$ (σ_y: yield stress and E: Young's modulus) The circles and the triangles show the case for $\alpha=0.8$ and 0.5. Each symbol applied black indicates that the column collapses in ten cycles of the sinusoidal acceleration. For $\alpha=0.8$ and $\lambda=60$, the column collapses when Z is over 9.0 m/s². If $\lambda\geqq90$, relatively smaller input acceleration amplitude leads to the collapse of the column, comparing to the case for $\lambda\leqq60$. In the case where $\lambda=90$ and $Z\geqq3.0$ m/s² or $\lambda\geqq120$ and $Z\geqq2.0$ m/s², the column collapses. This indicates that the dynamic strength of the column does not change with the slenderness ratio in the case for $\lambda\geqq90$. In the case where $\alpha=0.5$, the column does not collapse, if $\lambda\leqq90$ and $Z\leqq10.0$ m/s². The column collapses when $\lambda=120$, $Z\geqq7.0$ m/s² or $\lambda=150$, $Z\geqq5.0$ m/s². Therefore, it is found that the dynamic strength of the column is affected by the static axial compression force and that the smaller the slenderness ratio is, the more this effect is significant.

4. CONCLUSIONS

In this paper, the dynamic ultimate strength of columns with box sections subjected to the static axial compression force and the lateral sinusoidal acceleration is investigated using the numerical in-plane dynamic analysis. The main conclusions of this analysis is summarized as follows.

(1) When the column is subjected to combined the static axial force (actually a certain magnitude of the compression force) and the large lateral sinusoidal acceleration whose circular frequency is equal to the first natural circular

frequency of the column, the cross section in the vicinity of the midheight yields and the dynamic residual displacement increases only in one direction, diminishing the amplitude of the flexural vibration and the columns are brought out to collapse.

(2) When the columns subjected to the static axial compression force and the lateral sinusoidal acceleration collapse dynamically, the dynamic critical lateral deflection at midheight agrees with the static lateral deflection in the ultimate state.

(3) The columns which are subjected to ten cycles of the sinusoidal acceleration whose circular frequencies are equal to the first natural circular frequencies of the columns have relatively large dynamic ultimate strength, if the column has the slenderness ratio of $\lambda \leqq 60$. On the contrary, the dynamic strength decreases significantly, if the column is more slender than $\lambda = 90$. The dynamic ultimate strength does not change with the slenderness ratio in the case where $\lambda \geqq 120$.

(4) The dynamic ultimate strength of the columns decreases more remarkably in the case where the ratio of the applied static axial compression force to the load carrying capacity is equal to 0.8, than the case where the ratio is equal to 0.5. This indicates that the dynamic ultimate strength of the columns under the lateral sinusoidal acceleration is affected by the static axial compression force significantly. The smaller the slenderness ratio is, the more this effect is significant.

REFERENCES

1) Popov, E. P.: Seismic Behavior of Structural Subassemblages, ASCE, Vol. 106, ST7, pp. 1451～1474, July, 1980.
2) Suzuki, T. and K. Tamamatsu: Experimental Study on Energy Absorption Capacity of Columns of Low Steel Structures, Transaction of A.I.J., No. 279, pp. 65～75, May, 1975 (in Japanese).
3) Kato, B. and H. Akiyama: Energy Input and Damages in Structures Subjected to Severe Earthquakes, Transaction of A.I.J., No. 235, pp. 9～18, September, 1975 (in Japanese).
4) Kato, B. and H. Akiyama: Aseismic Limit Design of Steel Rigid Frames. Transaction of A.I.J., No. 237, pp. 59～65, November, 1975 (in Japanese).
5) Akiyama, H.: Aseismic Limit Design of Building Structures, Tokyo University Editions, 1980 (in Japanese).
6) Kawai, T.: Analysis of Stability Problems, Series in Structural Engineering by Computer II-6-B (Edited by Society of Steel Construction of Japan), Baifukan, 1974 (in Japanese).
7) Bathe, K. J., E. Ramm and E. L. Wilson: Finite Element for Large Deformation Dynamic Analysis, Int. Journal for Numerical Method in Engineering, Vol. 9, pp. 353～386, 1975.
8) Mizuta, Y., K. Nishiyama and I. Hirai: Phase Correction of Newmark's β-method, Proc. of JSCE, No. 268, pp. 15～21, December, 1977 (in Japanese).
9) Kuranishi, S. and T. Yabuki: In-plane ultimate strength of 2-hinged Steel Arches Subjected to Lateral Loads, Proc. of JSCE, No. 272, pp. 1～12, April, 1978 (in Japanese).
10) Premieniecki: Theory of Matrix Structural Analysis, McGraw-Hill, Inc., pp. 288～309, 1968.

(*Received June 17, 1983*)